

# Transfer Characteristic of $IM_3$ Relative Phase for a GaAs FET Amplifier

Noriharu Suematsu, *Member, IEEE*, Yoshitada Iyama, *Member, IEEE*, and Osami Ishida, *Senior Member, IEEE*

**Abstract**—The transfer characteristic of relative phase of the third-order intermodulation distortion ( $IM_3$ ) of a GaAs FET amplifier is measured and analyzed. The measurement system and method are also described. For drives in the weakly nonlinear region, the measured relative phase of  $IM_3$  is equal to that of the carrier and is in agreement with the analysis results using Volterra-series representation. For drives in the saturation region, the measured relative phase of  $IM_3$  versus the input power moves drastically compared with that of the carrier and is in agreement with numerical analysis using discrete Fourier transform. Comparison between measured and analytical results shows the drastic move of  $IM_3$  relative phase is caused by the generation of  $IM_3$  due to AM-PM conversion. The measured results and the measurement method are useful for the design and adjustment of predistortion-type linearizers for GaAs FET high-power amplifiers.

**Index Terms**—Amplifier distortion, intermodulation distortion, microwave FET amplifiers, microwave measurements, Volterra series.

## I. INTRODUCTION

BOOTH low-distortion and high-efficiency characteristics are desired for high-power amplifiers (HPA's) used in digital radio communication systems. In order to achieve both of them simultaneously, predistortion-type linearizing techniques have been used [1]–[5]. A predistortion-type radio frequency (RF) linearizer is connected to the input port of HPA and adds distortion components [mainly third-order intermodulation distortion ( $IM_3$ )] out of phase to the carrier. As a result, the distortion components generated in the linearizer and in the HPA are canceled out at the output port of the HPA. However, it is quite difficult to compensate the  $IM_3$  generated in the HPA operating near saturation [4]. Since the amplitude of  $IM_3$  generated in the linearizer can be easily adjusted to be equal to that in the HPA using a spectrum analyzer, it can be predicted that the phase of  $IM_3$  [6] generated in the HPA has moved drastically in the saturation region.

In this paper, the relative phase of  $IM_3$  versus the input power of a GaAs MESFET amplifier is measured and analyzed in two different methods. One is the analysis using Volterra-series representation [7]–[10], and the other is using discrete Fourier transform [11], [12]. The measurement system and method are also presented. Measured results show that: 1) for drives in the weakly nonlinear region the relative phase of  $IM_3$  is almost equal to that of carrier and 2) for drives

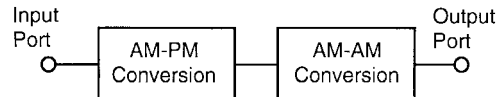


Fig. 1. Model of a nonlinear amplifier.

near saturation, the relative phase of  $IM_3$  moves drastically compared with that of carrier.

## II. ANALYSIS USING VOLTERRA-SERIES REPRESENTATION

In order to deduce the intermodulation characteristics for drive levels in the weakly-nonlinear region, Volterra-series analysis [7]–[10] is used. Taking into account the AM-PM conversion, the voltage transfer characteristics of a nonlinear amplifier can be obtained as follows.

A nonlinear amplifier can be modeled by two cascaded nonlinear elements, as shown in Fig. 1. One is a nonlinear phase element which represents AM-PM conversion of the nonlinear amplifier, and another is a nonlinear amplitude element which represents AM-AM conversion. For single-tone operation, the input voltage of this nonlinear amplifier  $v_{in}$  becomes

$$v_{in} = A \cos \omega t \quad (1)$$

where  $A$  and  $\omega$  are the voltage amplitude and the frequency of the input signal, respectively. The output voltage of the first nonlinear element (AM-PM)  $v_{im}$  can be written as

$$v_{im} = A \cos \left[ \omega t + \varphi \left( \frac{A^2}{2} \right) \right] \quad (2)$$

where  $\varphi(A^2/2)$  represents the AM-PM conversion. Using Volterra-series representation, the output voltage of the second nonlinear element (AM-AM)  $v_{out}$  can be written as

$$\begin{aligned} v_{out} &= \sum_{n=1}^{\infty} a_n v_{im}^n \\ &= \sum_{n=1}^{\infty} a_n A^n \cos^n \left[ \omega t + \varphi \left( \frac{A^2}{2} \right) \right]. \end{aligned} \quad (3)$$

In the case of two-tone ( $\omega_1, \omega_2$ ) operation, the input voltage  $v_{in}$  is

$$\begin{aligned} v_{in} &= A' \cos \omega_1 t + A' \cos \omega_2 t \\ &= 2A' \cos \frac{\omega_1 - \omega_2}{2} t \cdot \cos \frac{\omega_1 + \omega_2}{2} t \\ &= e(t) \cos \frac{\omega_1 + \omega_2}{2} t \end{aligned} \quad (4)$$

Manuscript received March 28, 1997; revised July 31, 1997.

The authors are with the Information Technology R&D Center, Mitsubishi Electric Corporation, Kanagawa 247, Japan.

Publisher Item Identifier S 0018-9480(97)08337-3.

where  $A'$  is the voltage amplitude of each input signal ( $\omega_1, \omega_2$ ) and  $e(t)$  is the component of the envelope, i.e.,

$$e(t) = 2A' \cos \frac{\omega_1 - \omega_2}{2} t. \quad (5)$$

$A$  and  $\omega$  in (1) in the case of two-tone operation can be expressed by using  $A'$ ,  $\omega_1$ , and  $\omega_2$ :

$$\begin{aligned} A &= e(t) \\ &= 2A' \cos \frac{\omega_1 - \omega_2}{2} t \end{aligned} \quad (6)$$

$$\omega = \frac{\omega_1 + \omega_2}{2}. \quad (7)$$

By substituting (6) and (7) for (1),  $\nu_{\text{out}}$  can be written as shown in (8), shown at the bottom of the page.

When  $(\nu_{\text{out}})_{\omega=\omega_x}$  is defined as the  $\omega = \omega_x$  component of  $\nu_{\text{out}}$ , the components of carrier ( $\omega = \omega_1$ ) and  $\text{IM}_3$  ( $\omega = 2\omega_2 - \omega_1$ ) can be derived from (8). The carrier ( $\omega = \omega_1$ ) component is

$$\begin{aligned} (\nu_{\text{out}})_{\omega=\omega_1} &= (a_1 A' + \frac{9}{4} a_3 A'^3 + \dots) \\ &\cdot \cos \left\{ \omega_1 t + \varphi \left[ \frac{e(t)^2}{2} \right] \right\} \end{aligned} \quad (9)$$

and the  $\text{IM}_3$  ( $\omega = 2\omega_2 - \omega_1$ ) component is

$$\begin{aligned} (\nu_{\text{out}})_{\omega=2\omega_2-\omega_1} &= (\frac{3}{4} a_3 A'^3 + \dots) \\ &\cdot \cos \left\{ (2\omega_2 - \omega_1) t + \varphi \left[ \frac{e(t)^2}{2} \right] \right\}. \end{aligned} \quad (10)$$

If the intermodulation distortion generation caused by AM-PM conversion can be neglected,  $\cos \{ \omega_x t + \varphi [e(t)^2/2] \}$  would not make any intermodulation distortion components. Therefore, (9) and (10) show that, when the generation of  $\text{IM}_3$  caused by AM-PM conversion is negligibly small compared with that caused by AM-AM conversion, the carrier and  $\text{IM}_3$  have the same relative phase characteristic versus the input power  $e(t)^2/2$ .

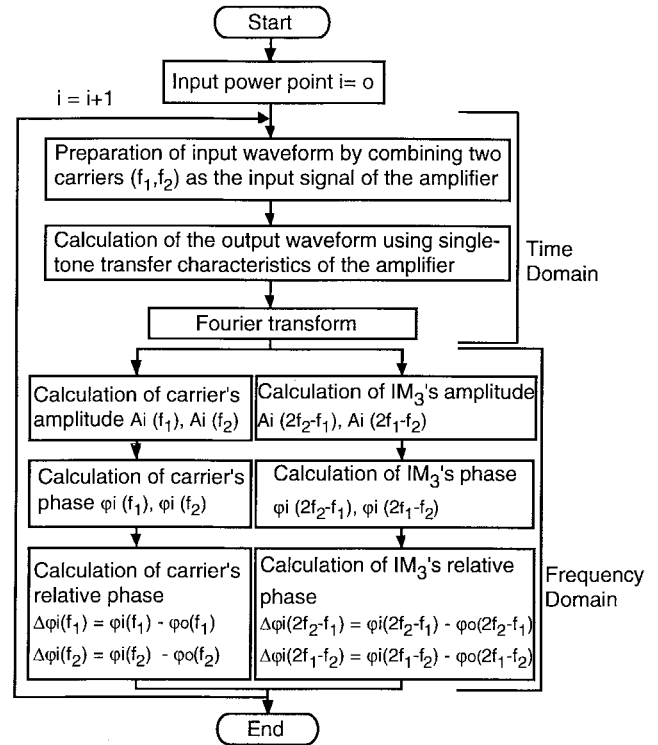


Fig. 2. Flow chart of the calculation of the input power dependence of the amplitude and relative phases of carrier and  $\text{IM}_3$  in the case of two-tone.

### III. NUMERICAL ANALYSIS USING DISCRETE FOURIER TRANSFORM

In order to take into account the effect of  $\text{IM}_3$  generation caused by AM-PM conversion, numerical analysis using the discrete Fourier transform [11], [12] can be adopted. The calculation of relative phase of carrier and  $\text{IM}_3$  is added to the previous analysis [12]. The flow chart of this calculation is shown in Fig. 2. In this method, the waveform of the

$$\begin{aligned} \nu_{\text{out}} &= \sum_{n=1}^{\infty} a_n \left( e(t) \cos \left\{ \frac{\omega_1 + \omega_2}{2} t + \varphi \left[ \frac{e(t)^2}{2} \right] \right\} \right)^n \\ &= a_1 A' \left( \cos \left\{ \omega_1 t + \varphi \left[ \frac{e(t)^2}{2} \right] \right\} + \cos \left\{ \omega_2 t + \varphi \left[ \frac{e(t)^2}{2} \right] \right\} \right) \\ &\quad + a_2 A'^2 \left( \frac{1}{2} \cos \left\{ 2\omega_1 t + 2\varphi \left[ \frac{e(t)^2}{2} \right] \right\} + \frac{1}{2} \cos \left\{ 2\omega_2 t + 2\varphi \left[ \frac{e(t)^2}{2} \right] \right\} \right. \\ &\quad \left. + \cos \left\{ (\omega_1 + \omega_2) t + 2\varphi \left[ \frac{e(t)^2}{2} \right] \right\} + \cos [(\omega_1 - \omega_2) t] + 1 \right) \\ &\quad + a_3 A'^3 \left( \frac{1}{4} \cos \left\{ 3\omega_1 t + 3\varphi \left[ \frac{e(t)^2}{2} \right] \right\} + \frac{1}{4} \cos \left\{ 3\omega_2 t + 3\varphi \left[ \frac{e(t)^2}{2} \right] \right\} \right. \\ &\quad \left. + \frac{3}{4} \cos \left\{ (2\omega_1 + \omega_2) t + 3\varphi \left[ \frac{e(t)^2}{2} \right] \right\} + \frac{3}{4} \cos \left\{ (2\omega_2 + \omega_1) t + 3\varphi \left[ \frac{e(t)^2}{2} \right] \right\} \right. \\ &\quad \left. + \frac{9}{4} \cos \left\{ \omega_1 t + \varphi \left[ \frac{e(t)^2}{2} \right] \right\} + \frac{9}{4} \cos \left\{ \omega_2 t + \varphi \left[ \frac{e(t)^2}{2} \right] \right\} \right. \\ &\quad \left. + \frac{3}{4} \cos \left\{ (2\omega_1 - \omega_2) t + \varphi \left[ \frac{e(t)^2}{2} \right] \right\} + \frac{3}{4} \cos \left\{ (2\omega_2 - \omega_1) t + \varphi \left[ \frac{e(t)^2}{2} \right] \right\} \right) \\ &\quad + \dots \end{aligned} \quad (8)$$

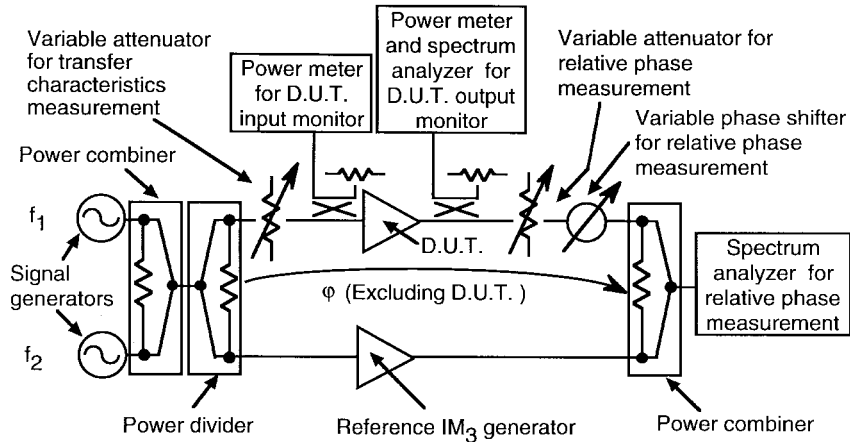


Fig. 3. Configuration of measurement system for input power dependence of relative phase of  $IM_3$ .

input signal is modulated in the time domain by using the measured single-tone transfer characteristic (AM-AM and AM-PM conversion) of the amplifier, then transferred into the frequency domain by using the discrete Fourier transform [12]. In the frequency domain, amplitude and phase of carrier and  $IM_3$  are calculated, then the relative phase is derived from the calculated phase. By using this numerical analysis, the generation of  $IM_3$  due to AM-PM conversion can be considered as well as that due to AM-AM conversion.

#### IV. MEASUREMENT SYSTEM AND METHOD

Fig. 3 shows the configuration of measurement system. Two carriers (2500 and 2501 MHz) generated in two independent oscillators are combined and then divided into two paths. One is connected to an amplitude transfer characteristics measurement system including device under test (DUT), and another to a reference  $IM_3$  generator. The input power of the amplifier for reference  $IM_3$  generation is kept constant to generate distortion independent of the input power of the DUT. The output of the amplitude transfer characteristics measurement system is connected to a variable attenuator and a variable phase shifter, then is combined with the output of the reference  $IM_3$  generator, and finally connected to a spectrum analyzer. The phase change through the path of the amplitude transfer characteristics measurement system excluding the DUT is defined as  $\varphi$ .

The relative phase of carrier and  $IM_3$  are measured by the following procedure. At the first stage ( $i = 0$ ,  $i$ : number of the stage), at where the input power level is set in the weakly nonlinear region of the DUT, the phase standards of carrier and  $IM_3$  are measured. In order to measure the phase standard of carrier, the variable attenuator and the variable phase shifter are adjusted to minimize the spectral intensities of the two carrier components monitored by the spectrum analyzer. Fig. 4 shows the monitored spectrum under the measurement of phase of carrier. Here  $\varphi$  is defined as the phase standard of the carrier  $\varphi_{C0}$ . To measure the phase standard of  $IM_3$ , the attenuator and the phase shifter are adjusted to minimize the spectral intensities of  $IM_3$ . Fig. 5 shows the monitored spectrum under the measurement of phase of  $IM_3$ . Here  $\varphi$

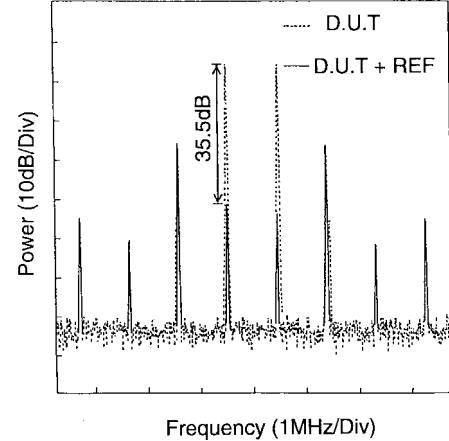


Fig. 4. Spectrum under measurement of relative phase of the carrier.

is defined as the phase standard of  $IM_3$ . Since there are two components of  $IM_3$  (that is, 2499 and 2502 MHz), the phase standards of  $IM_3$  are defined as  $\varphi_{L0}$  and  $\varphi_{H0}$ , respectively. Then, the same measurement procedure is repeated at the next input power level, and the phase of carrier and  $IM_3$  ( $\varphi_{Ci}$ ,  $\varphi_{Li}$ , and  $\varphi_{Hi}$ ) can be obtained for the  $i$ th stage ( $i > 0$ ). The relative phase of carrier ( $\Delta\varphi_{Ci}$ ) and the relative phase of  $IM_3$  ( $\Delta\varphi_{Li}$  and  $\Delta\varphi_{Hi}$ ) versus input power are defined as  $\varphi_{Ci} - \varphi_{C0}$ ,  $\varphi_{Li} - \varphi_{L0}$ , and  $\varphi_{Hi} - \varphi_{H0}$ , respectively.

During this measurement, the variable attenuator and the variable phase shifter are adjusted to attain 30-dB suppression for both carrier and  $IM_3$ . Fig. 6 shows the relationship between signal suppression and differential power and phase of two input signals combined at  $180^\circ$  out of phase to cancel each other. When the differential power between two signals is zero, 35.5- and 29.0-dB signal suppression, shown in Figs. 4 and 5, are equivalent to  $\pm 1.3^\circ$  and  $\pm 2.0^\circ$  measurement phase error, respectively.

#### V. MEASURED RESULTS

The characteristics of a 2.5-GHz-band class-A amplifier, using a GaAs MESFET (MGFC2407A, Mitsubishi Electric), were measured. Fig. 7 shows the single-tone transfer char-

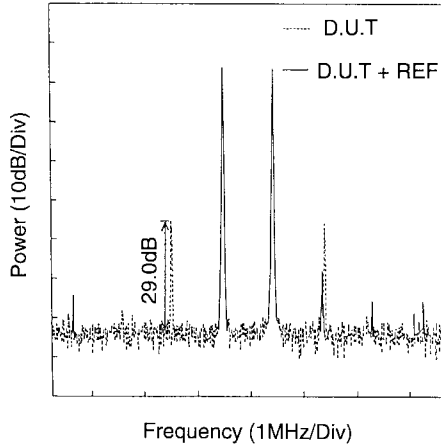


Fig. 5. Spectrum under measurement of relative phase of  $IM_3[2f_1 - f_2 (f_2 > f_1)]$ .

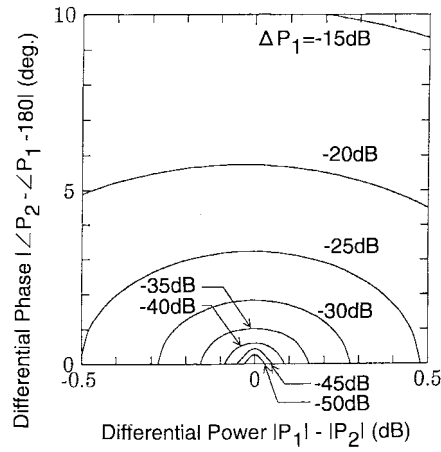


Fig. 6. Relationship between signal suppression  $\Delta P_1$  and differential power and phase of two input signals ( $P_1$  and  $P_2$ ) combined at  $180^\circ$  out of phase.

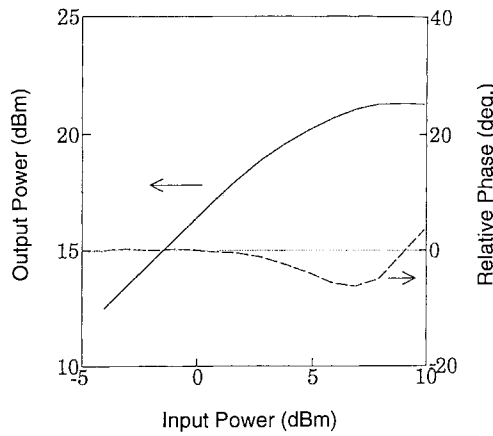


Fig. 7. Single-tone transfer characteristics of GaAs MESFET amplifier.

acteristics of the amplifier. The output power at 1-dB gain compression ( $P_1$  dB) is about 19 dBm, and the relative phase of carrier is less than  $5^\circ$  below  $P_1$  dB.

Fig. 8 shows the measured two-tone amplitude transfer characteristics. Below the input power of 0 dBm, the amplitude of  $IM_3$  rapidly decreases and is less than  $-30$  dBm. In this

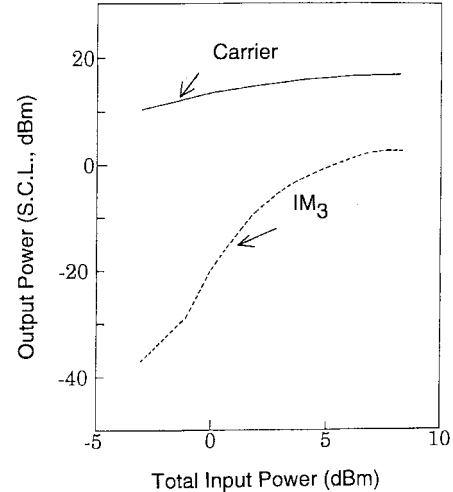


Fig. 8. Measured input power dependence of output power of carrier and  $IM_3$  in the case of two-tone characteristics.

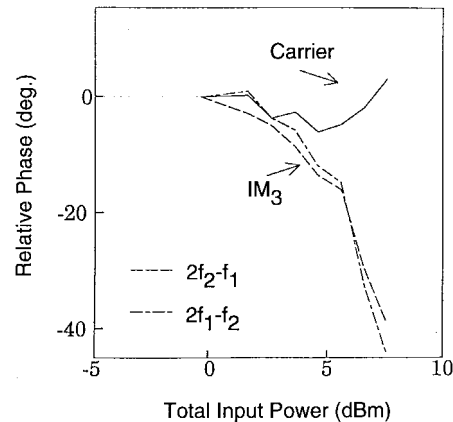


Fig. 9. Measured input power dependence of relative phase of carrier and  $IM_3$  in the case of two tones.

region, since the power level difference between  $IM_3$  and noise, monitored at the spectrum analyzer, is small, enough suppression cannot be achieved for the phase measurement of  $IM_3$ . Therefore, the input power of the DUT at the first stage of relative phase measurement is set to 0 dBm. Fig. 9 shows the measured relative phase of carrier and  $IM_3$  versus input power.

By comparing Fig. 9 with Fig. 7, the magnitude of relative phase of carrier in the case of two tones is nearly equal to that in the case of a single tone, but the locus in the case of two tones is about 2 dB shifted toward lower input power (note that the abscissa of Fig. 9 is total input power). In the case of two tones, even though the average power is equal to that in the case of a single tone, the peak power of combined waveform of two carrier is about 3 dB higher than that of single carrier. In a weakly nonlinear region, the relative phase of  $IM_3$  is almost equal to that of carrier. For drives near saturation, the relative phase of  $IM_3$  is quite larger than that of carrier, and the relative phase of  $IM_3$  exceeded  $30^\circ$  whereas the relative phase of carrier moved below  $5^\circ$ .

The analysis shown in Section II, in which the generation of  $IM_3$  due to AM-PM conversion is neglected, shows that

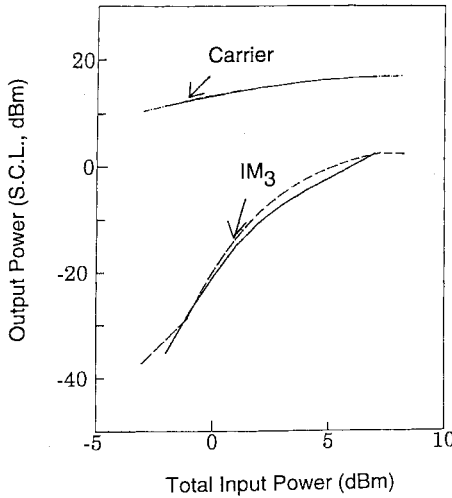


Fig. 10. Calculated input power dependence of the output power of carrier and  $IM_3$  in the case of two tones. Solid lines show the measured results and dotted lines show the calculated results.

the relative phase of carrier and  $IM_3$  should be equal. In the weakly nonlinear region, since the measured result is in agreement with the analysis result shown in Section II, the generation of  $IM_3$  would be mainly due to AM-AM conversion.

The calculation of amplitude and relative phase characteristics is carried out by using numerical analysis described in Section III. Fig. 10 shows the calculated output power of the carrier and the  $IM_3$  versus the input power in the case of two tones. Fig. 11 shows the relative phase of the carrier and the  $IM_3$ . In both figures, the solid lines represent the calculated results, and the dotted lines represent the measured results shown in Figs. 8 or 9, previously. The amplitude difference between the calculated and the measured  $IM_3$  is less than 2 dB, and the relative phase difference between the calculated and the measured  $IM_3$  is less than  $4^\circ$ . Both measured and calculated characteristics show the rapid phase change of the  $IM_3$  for drives near saturation. This result indicates that in the saturation region the generation of  $IM_3$  due to AM-PM conversion should also be considered, and it causes the drastic move of the relative phase of  $IM_3$ .

## VI. CONCLUSION

The relative phase of  $IM_3$  versus input power of a GaAs MESFET amplifier was measured and analyzed. The measurement system and method were also presented. Measured results of the GaAs MESFET amplifier demonstrated that the characteristics of the relative phase of carrier versus input power in the case of two tones had similar locus to that in the case of a single tone. For drives in weakly nonlinear region, the relative phase of  $IM_3$  is almost equal to that of carrier as predicted in the analysis using Volterra-series representation. For drives near saturation, the relative phase of  $IM_3$  is much larger than that of the carrier and is in agreement with the result of numerical analysis using discrete Fourier transform. Near saturation region, the relative phase of  $IM_3$  exceeds  $30^\circ$ , whereas the relative phase of carrier moves less than  $5^\circ$ .

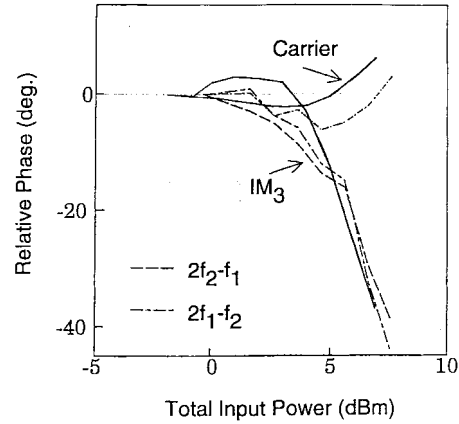


Fig. 11. Calculated input power dependence of the relative phase of carrier and  $IM_3$  in the case of two tones. Solid lines show the measured results and dotted lines show the calculated results.

Comparison between measured and analytical results indicates that in the weakly nonlinear region, the generation of  $IM_3$  is mainly due to AM-AM conversion, whereas in the saturation region, the generation of  $IM_3$  due to AM-PM conversion cannot be neglected with that due to AM-AM conversion. This means that the drastic move of the relative phase of  $IM_3$  is caused by the  $IM_3$  generation due to AM-PM conversion.

It had been previously predicted that the drastic move of the relative phase of  $IM_3$  versus the input power occurred for GaAs MESFET amplifiers operating near saturation, because of the difficulties in the adjustment of predistortion-type RF linearizers. The measured results and the measurement method presented here are useful in the design and the adjustment of these linearizers. If an HPA having zero AM-PM conversion characteristic can be achieved, it might have zero relative phase of  $IM_3$  versus the input power. Therefore, it would not be difficult for a predistortion-type linearizer to compensate  $IM_3$  of the HPA even in the saturation region.

## REFERENCES

- [1] N. Imai, T. Nojima, and T. Murase, "Novel linearizer using balanced circulators and its application to multilevel digital systems," *IEEE Trans. Microwave Theory Tech.*, vol. 37, pp. 1237-1243, Aug. 1989.
- [2] G. Satoh, "MIC linearizer for satellite communications," *Trans. IECE Japan*, vol. J67-B, no. 6, pp. 630-637, June 1984.
- [3] R. Inada, H. Ogawa, S. Kitazume, and P. Desantis, "A compact 4-GHz linearizer for space use," *IEEE Trans. Microwave Theory Tech.*, vol. MTT-34, pp. 1327-1332, Dec. 1986.
- [4] N. Suematsu, T. Takagi, A. Iida, and S. Urasaki, "A predistortion type equi-path linearizer in Ku-band," in *3rd Asia-Pacific Microwave Conf. Proc.*, 1990, pp. 1077-1080.
- [5] K. Yamauchi, K. Mori, M. Nakayama, Y. Itoh, Y. Mitsui, and O. Ishida, "A novel series diode linearizer for mobile radio power amplifiers," in *IEEE MTT-S Dig.*, 1996, pp. 831-834.
- [6] T. Yoshida, K. Monma, and K. Morita, "Self cancellation type low distortion balanced amplifiers," *IECE, Tech. Rep.*, vol. MW76-140, pp. 49-54, 1976.
- [7] R. J. Westcott, "Investigation of multiple f.m./f.d.m. carriers through a satellite t.w.t. operating near to saturation," *Proc. IEE*, vol. 114, no. 6, pp. 726-740, June 1967.
- [8] R. S. Tucker, "Third-order intermodulation distortion and gain compression in GaAs FET's," *IEEE Trans. Microwave Theory Tech.*, vol. MTT-27, pp. 400-408, May 1979.

- [9] T. Nojima and Y. Okamoto, "Analysis and compensation of TWT nonlinearities based on complex power series representation," *Trans. IECE Japan*, vol. J64-B, no. 12, pp. 1449-1456, Dec. 1981.
- [10] S. Ohwaku and D. Kuwagaki, "Common amplification of many signals by traveling wave tube amplifier," *Trans. IECE Japan*, vol. J51-B, no. 5, pp. 193-200, May 1968.
- [11] G. R. Stette, "Calculation of intermodulation from a single carrier amplitude characteristics," *IEEE Trans. Commun.*, vol. COMM-22, pp. 319-323, Mar. 1974.
- [12] T. Takagi, S. Ogura, Y. Ikeda, and N. Suematsu, "Intermodulation and noise power ratio analysis of multiple-carrier amplifiers using discrete Fourier transform," *Trans. IECE Japan*, vol. E77-C, no. 6, pp. 935-941, June 1994.



**Noriharu Suematsu** (M'92) received the B.S. and M.S. degrees in electronics and communication engineering from Waseda University, Tokyo, Japan, in 1985 and 1987, respectively.

In 1987, he joined Mitsubishi Electric Corporation, Kanagawa, Japan, where he has been engaged in research and development of microwave and millimeter-wave solid state circuits. During 1992-1993, he was a Visiting Researcher at the University of Leeds, U.K.

Mr. Suematsu is a member of the Institute of Electronics, Information, and Communication Engineers of Japan (IEICE) and the Japan Society of Applied Physics. In 1991, he received the Shinohara Award from the IEICE.



**Yoshitada Iyama** (M'94) received the B.S., M.S., and Dr. Eng. degrees in electronic engineering from Tohoku University, Sendai, Japan, in 1978, 1980 and 1997, respectively.

In 1980, he joined Mitsubishi Electric Corporation, Kanagawa, Japan, where he has been engaged in research and development of microwave control circuits and monolithic microwave integrated circuits.

Dr. Iyama is a member of the Institute of Electronics, Information, and Communication Engineers.



**Osami Ishida** (M'89-SM'95) received the B.S. and M.S. degrees in electronic engineering and the Dr.Eng. degree from Shizuoka University, Hamamatsu, Japan, in 1971, 1973, and 1992, respectively.

In 1973, he joined Mitsubishi Electric Corporation, Kanagawa, Japan. He was a Manager in the Aperture Antenna Group from 1988 to 1992, Deputy Manager in the Opto and Microwave Electronics Department from 1993 to 1995, and is presently a Manager in the Microwave Electronics Department at the Information Technology R&D Center. He has been engaged in research and development of microwave circuit technologies in antenna feeds for satellite communication and phased array radars and in devices for mobile communication.

Dr. Ishida is a member of the Institute of Electronic, Information, and Communication Engineers (IEICE), and served as a member of the Editorial Committee for the *Transactions of IEICE* from 1988 to 1992.